ORIGINAL ARTICLE

Functional Connectivity Assessment in Alzheimer's Disease: A Comparative Study of Linear and Non-linear fMRI Analysis Approaches

Hessam Ahmadi [1], Emad Fatemizadeh [2*], Ali Motie-Nasrabadi [3]

[1] *Department of Biomedical Engineering, Science and Research Branch, Islamic Azad University, Tehran, Iran*

[2] *School of Electrical Engineering, Sharif University of Technology, Tehran, Iran*

[3] *Biomedical Engineering Department, Shahed University, Tehran, Iran*

*Corresponding Author: Emad Fatemizadeh
Email: fatemizadeh@sharif.edu

Received: 24 December 2024 / Accepted: 18 February 2025

Abstract

Purpose: Brain connectivity studies unveil the intricate interactions within neural networks. Various approaches exist to explore brain connectivity, yet the debate between the efficacy of linear versus non-linear methods remains unresolved due to the advantages and limitations of each.

This study aims to provide a comprehensive evaluation of neuroimaging data analysis to gain insights into the functional aspects of the brain, particularly in the context of Alzheimer's Disease (AD). The objective is to identify potential pathways for early intervention and prevention, despite the controversies arising from diverse neuroimaging modalities and analytical techniques.

Materials and Methods: Using fMRI data, both linear and non-linear approaches are investigated. The linear approach employs the Pearson Correlation Coefficient (PCC) to create whole-brain graphs. For non-linear approaches, Distance Correlation (DC) and the kernel trick are utilized. Functional brain networks are constructed and sparsified for each AD stage, followed by calculating global graph measures.

Results: The findings indicate that non-linear approaches are more effective in distinguishing between different stages of AD. Among these, the kernel trick method performs better than the DC technique. Polynomial kernel (degree 3) showed better group separability, with significantly different graph measures such as clustering, transitivity, modularity, and small-worldness. Kernel analysis revealed that within-region connectivity was more disrupted in AD. Notably, the functional graphs of the brain are more significantly degraded in the early stages of AD.

Conclusion: In the initial phases of AD, both functional integration and segregation of the brain are compromised, with a more pronounced decline in functional segregation as the disease progresses. The clustering coefficient, indicative of brain functional segregation, emerges as the most distinguishing feature across all stages of AD, highlighting its potential as a biomarker for early diagnosis.

Keywords: functional Magnetic Resonance Imaging; Functional Connectivity; Linear Analysis; Graph Theory; Alzheimer's Disease; Non-Linear Dynamics.

DOI: https://doi.org/10.18502/fbt.v12i3.19171

1. Introduction

Neurological diseases affect brain behavior and cognitive function noticeably. Alzheimer's Disease (AD) is a destructive and progressive neurological disease discovered in 1906 by Dr. Alois Alzheimer. Although more than a century has passed since the first AD case, there is still no definitive and effective treatment. Studies have shown that AD progresses through different stages, including Early Mild Cognitive Impairment (EMCI) and Late Mild Cognitive Impairment (LMCI), and it may take up to a decade for acute clinical symptoms to appear [1]. Since there is no specific treatment to return the patient to normal mental health, early detection is vital. Several experiments have revealed that the brain suffers from atrophy in AD [2].

The investigation of neurological diseases' effects on the brain has garnered significant attention from researchers. While structural changes in the brain have been extensively studied through imaging techniques such as Computed Tomography (CT) and Magnetic Resonance Imaging (MRI), the impact of these diseases on brain function has been less clear. In recent decades, methods like functional MRI (fMRI) and Positron Emission Tomography (PET) have increased the focus on brain function studies. fMRI, in particular, involves multiple MRI scans performed every few seconds to monitor changes in brain oxygen consumption, capturing low-frequency oscillations known as Blood-Oxygen-Level-Dependent (BOLD) signals [3]. Although brain behavior remains a topic of debate, some researchers model and analyze the brain as a linear system. However, this approach is overly simplistic, and non-linear methods offer a closer approximation of the brain's inherent complexity.

A common tool to analyze fMRI signals is graph theory. In this approach, brain regions or voxels are modeled as graph nodes, and the links between the nodes are made using fMRI signals. Consequently, the edges represent the relationships between brain regions. Among various methods, the Pearson Correlation Coefficient (PCC) is the most widely used approach to modeling brain functional connectivity. PCC measures the correlation between two fMRI signals, yielding a value between -1 and 1. The sign indicates the direction of the connectivity, while the magnitude reflects its strength [4]. However, PCC captures only the linear dependency between two time series, which is an oversimplification of the brain's complex relationships. Ample research shows that the brain's signals, including fMRI, demonstrate non-linear behavior. Despite this, PCC remains a widespread and reliable method for brain functional connectivity analysis [5]. A study on a non-linear alternative to PCC based on fMRI time series of Alzheimer's Disease (AD) was conducted. This study utilized the kernel trick, a polynomial kernel, to increase the dimensionality of the input space and perform PCC calculations in this new space, making the PCC in the new space equivalent to non-linear relations in the primary space [6], Another study employed Kernel Canonical Correlation (KCC) to analyze fMRI and EEG data [7]. Amidst ongoing debates about linear versus non-linear methods, Gabor introduced Distance Correlation (DC) to overcome PCC's limitations in capturing non-linear dependencies. DC quantifies both linear and non-linear dependencies between two signals [8]. The results indicate that DC is more powerful than PCC for measuring the relationship between two vectors. While deep learning methods have significantly improved classification and clustering accuracies for both linear and non-linear approaches, grasping the underlying cognitive neuroscience behavior remains critical [9, 10]. Regardless of the high accuracies achieved, it is important to determine whether linear or non-linear methods better model this behavior [11]. In the literature, patients are often classified from normal subjects based on structural changes in the brain [12]. Additionally, several biomarkers have been identified [13]. A recent study examines different deep learning architectures to perform a binary classification of AD based on structural MRI data. The models were divided into two categories: with and without augmentation. Results show that the Convolutional Neural Networks and Long Short-Term Memory (CNN-LSTM) were superior and reached more than 99.9% accuracy [14]. Khazaee et al. utilized functional connectivity information to distinguish AD subjects and predict conversion from MCI to AD, achieving more than 96% accuracy [15]. A study was focused on fMRI data to distinguish MCI and AD from control subjects. By employing Principle Component Analysis (PCA) the feature space dimension was reduced. They proposed a kernel-based

PCA Support Vector Regression (SVR) and achieved 98.53% accuracy [16]. In [17] authors performed a classification among 4 different stages of AD (Normal-EMCI-LMCI and AD) based on functional data. They employed U-Net architecture to extract spatial features, and the LSTM to extract temporal features. By a 5-fold cross-validation, the deep network demonstrates 96.4% accuracy on average. Another interesting approach is combining structural data with functional data to gain a generalized insight into AD, which achieved 56% accuracy for three-class classification [18].

Linear methods, such as the Pearson Correlation Coefficient (PCC), are widely used for their simplicity but are limited to capturing linear dependencies and may overlook the complex, non-linear interactions inherent in neural systems. Non-linear methods, such as Distance Correlation (DC) and kernel-based approaches, address this limitation by capturing higher-order relationships, providing deeper insights into the subtle connectivity changes associated with Alzheimer's Disease (AD). As mentioned before, most studies have used PCC to generate brain graphs or utilized non-linear approaches individually. Although some studies, such as [19] compare different correlation methods, no study has combined PCC with robust non-linear methods such as DC and kernel-based approaches. Understanding how brain functional connectivity evolves with AD progression is crucial, as it could pave the way for more effective early detection strategies and therapeutic interventions. Several studies have used both linear and non-linear approaches [20]. In the present study, to address the limitations of previous analyses, PCC is employed as the most accepted linear method, alongside kernel-based and DC methods as non-linear tools to analyze fMRI data of AD. Furthermore, to consider the gradual nature of AD and ensure a comprehensive experiment, three distinct conditions are explored: Healthy subjects vs. EMCI, EMCI vs. LMCI, and LMCI vs. AD. This study aims to investigate modifications in brain functional graphs as AD progresses.

The rest of the article is arranged as follows: In the materials and methods section, the fMRI data are introduced and the steps of preprocessing are described. Then, there is a sub-section called Correlation Methods, which consists of PCC, kernel-based, and DC definitions and relative equations. Afterwards, graph theory and statistical tests are described. In the Results section, the outcomes of analyses are elaborately reported. In the Discussion, the results are interpreted. Finally, concluding remarks are presented in the last section.

2. Materials and Methods

In this section, the utilized data and tools are presented separately, and each of them is explained completely. The research steps are summarized in Figure 1 as a block diagram.

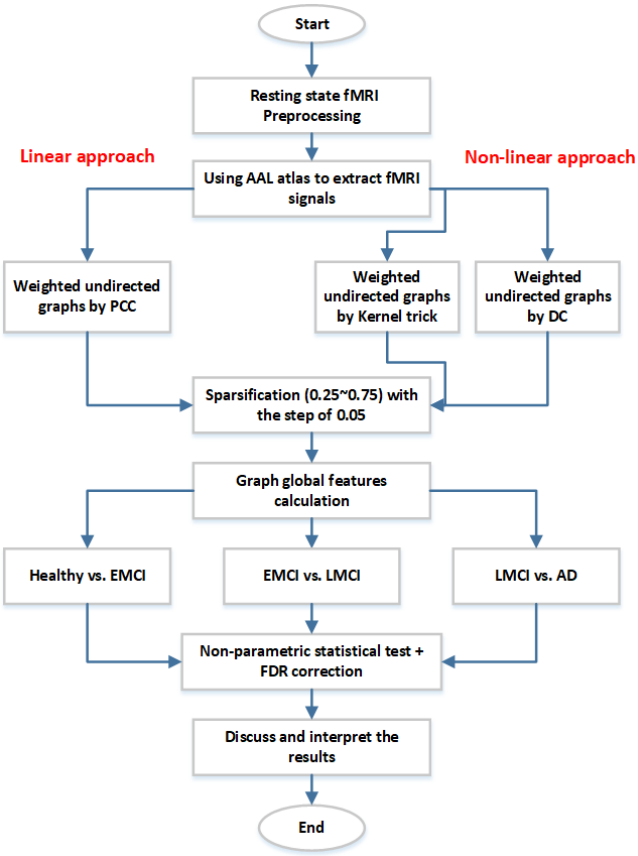

Figure 1. The research flowchart. (AAL: Automated Anatomical Labeling, PCC: Pearson Correlation Coefficients, DC: Distance Correlation, EMCI: Early Late Mild Cognitive Impairments, LMCI: Late Mild Cognitive Impairments, FDR: False Discovery Rate)

2.1. Data and Preprocessing

The fMRI data were collected from the second phase of the Alzheimer's Disease Neuroimaging Initiative (ADNI) project, which contains healthy subjects and all stages of AD (EMCI, LMCI, AD)

[21]. The selected cases are age-matched, and the mental examination scores, including Mini-Mental State Examination (MMSE) and Clinical Dementia Rating (CDR), were checked. Each fMRI data set contains 140 volumes with a Repetition Time (TR) of 3000 msec. The Echo Time (TE), flip angle, and slice thickness were 30 msec, 80 degrees, and 3.3125 mm, respectively.

For preprocessing the data, according to ADNI, there was no need to remove the first time points. The rest of the preprocessing steps were implemented as depicted in Figure 2. Data Processing Assistant for Resting-State fMRI (DPARSF) [22] was used for preprocessing, and Automated Anatomical Labeling (AAL) [23] was employed to extract Regions of Interest (ROI) signals. The AAL atlas contains 116 different ROIs that cover the whole brain, and in this study, all of them are employed for further processing. All other processing was conducted utilizing Matlab 2018a software.

2.2. Correlation Methods

2.2.1. Pearson Correlation Coefficient (PCC)

In statistics, correlation coefficients are used to measure the dependency between two vectors. PCC is the most popular method for this assessment but only addresses the linear relationship. If two variables have a total positive correlation, the PCC is +1, and -1 corresponds to a total negative correlation. A value of 0 exhibits no correlation. The PCC formula is (Equation 1):

$$\rho_{X_i.X_j} = \frac{\mathrm{cov}(X_i.X_j)}{\sigma_{X_i}\sigma_{X_j}} \quad (1)$$

Where σ_{X_i} and σ_{X_j} are the representative of the standard deviation of vectors X_i and X_j. Also Cov is the covariance of the vectors [24].

2.2.2. Kernel Trick and PCC

In the kernel trick, by using kernel functions, the input data is mapped to a new space. The linear calculations in the new space are equivalent to the non-linear computations in the primary space [25, 26]. Assuming that the data is x and the φ is the corresponding transformation, the kernel trick is as follows (Equation 2):

$$K(x_i, x_j) = x_i^T x_j$$
$$\varphi: x \rightarrow \varphi(x) \quad (2)$$
$$K(x_i, x_j) = \varphi(x_i)^T \varphi(x)$$

Where φ is the nonlinear transformation, x_i, x_j are the two variables, and K is the kernel function. According to the Mercer theorem, K has to be a positive definite [27]. By the use of $\varphi(x)$ the kernel trick, one can evaluate the inner product of two signals without knowing the $\varphi(x)$ [28].

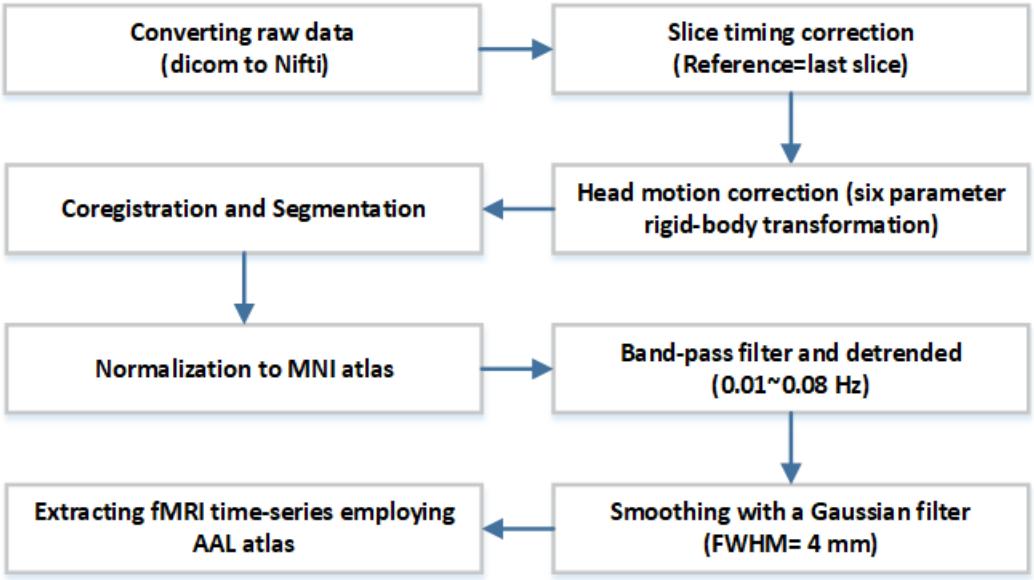

Figure 2. The preprocessing steps. MNI Montreal Neurological Institute, FWHM: Full with at Half Maximum

If X_i and X_j. are two signals, the covariance between them is defined as (Equation 3):

$$\mathrm{cov}(X_i.X_j) = (X_i - \mu).(X_j - \vartheta) \quad (3)$$

where μ and ϑ are the means of two X_i and X_j signals respectively and '.' is the dot product. The above covariance is the Pearson Covariance [29]. Now, the PCC is defined as [29] (Equation 4):

$$\rho_{X_i.X_j} = \frac{\mathrm{cov}(X_i.X_j)}{\sqrt{\mathrm{cov}(X_i.X_i)\mathrm{cov}(X_j.X_j)}} \quad (4)$$

Consequently, the PCC is rewritten regarding the dot product; therefore, based on [30] the kernel trick is applicable as follows (Equation 5):

$$K\left\{\rho_{X_i.X_j}\right\} = \frac{K\{(X_i.X_j)\}}{\sqrt{K(X_i.X_i)K(X_j.X_j)}} \quad (5)$$

As shown, the PCC cannot uncover nonlinear relationships. Therefore, rather than calculating the PCC in the primary space, the kernel trick is utilized to process the PCC in the new space. This approach captures nonlinear relationships in the primary space. "The polynomial kernel (degree 3) was selected based on its demonstrated effectiveness in capturing non-linear dependencies in brain connectivity, as highlighted in the paper [7]. Alternative kernels, such as Gaussian and sigmoid, were considered. However, their performance was found to be less robust in detecting functional connectivity changes, as observed in earlier research [7]. Consequently in this study, based on [6], the polynomial kernel function was selected. It is worthwhile mentioning that while kernel performance can vary, kernels such as Gaussian or sigmoid may require intensive parameter tuning, which could affect the precision of findings. Using a less suitable kernel might weaken group separability or reduce statistical significance in detecting connectivity changes.

2.2.3. Distance Correlation (DC)

Based on the limitations of PCC for the evaluation of non-linear dependencies, DC was introduced to quantify non-linear relationships [8]. Assuming that $(X_m, Y_m, m = 1,2,\dots m,n)$ are two vectors. In this method, the distance matrix is defined as:

$$a_{e,f} = \|X_e - X_f\|, e, f = 1,2,\dots,n$$
$$b_{e,f} = \|Y_e - Y_f\|, e, f = 1,2,\dots,n \quad (6)$$

Where $\| \ \|$ is the Euclidean distance. Also, $A_{e,f}$ and $B_{e,f}$ can be described as (Equation 7):

$$A_{e,f} = a_{e,f} - \overline{a_{e.}} - \overline{a_{f.}} + \overline{a_{..}}$$
$$B_{e,f} = b_{e,f} - \overline{b_{e.}} - \overline{b_{f.}} + \overline{b_{..}} \quad (7)$$

Where $\overline{a_{e.}}$ is the mean of the e^{th} row and $\overline{a_{f.}}$ is the mean of the f^{th} column. The mean correlation distance is $\overline{a_{..}}$. B and A are defined identically. Finally, the arithmetic average of the product of $A_{e,f}$ and $B_{e,f}$ is the distance covariance (Equation 8):

$$dCov_n^2(X,Y) = \frac{1}{n^2}\sum_{e=1}^{n}\sum_{f=1}^{n} A_{e,f}B_{e,f} \quad (8)$$

Accordingly, the DC is defined as (Equation 9):

$$dCor(X,Y) = \frac{dcov(X,X)}{\sqrt{dVar((X)dVar(Y)}} \quad (9)$$

Where dVar is distance variance and computed similarly to dCov as mentioned above.

2.3. Graph Theory

Regardless of whether the analysis is region-based or voxel-based, fMRI processing involves large datasets. Given the large number of voxels or regions available, calculating the correlation among all pairwise combinations provides a significant amount of information. A practical approach to managing this complexity is graph theory. In this context, nodes in the graph represent brain regions or voxels, and the edges represent functional or effective connectivity. $G = (V, E)$ is used to represent a graph, where V denotes the nodes (brain regions) and E denotes the edges (connectivity) [31]. To eliminate weak and spurious edges that do not reflect real and strong correlations in the brain, a sparsification step is performed. This step converts weighted graphs into binarized ones [32]. Given that identifying an optimal threshold is still controversial, this research explores functional graphs with thresholds ranging from 0.25 to

0.75, in steps of 0.05, for a comprehensive investigation.

By employing graph theory, various measures can be defined to reflect the characteristics of the brain graph. A healthy brain network demonstrates functional integration and segregation, which allow information to flow efficiently and flexibly. Neurological diseases such as AD degrade brain networks and impair these properties. The utilized graph features are introduced in Table 1. Please note that the small-world property of the brain was verified before calculating the features.

n is the number of nodes, l is the number of links, and $d_G(x,y)$ is the distance between the x and$y$. G^{FC} is a representative of a fully connected graph. $A_{x,y}$ shows the connectivity matrix. The $\delta_{x,y}$ is 0 if the two vertices are from one module, otherwise, it is 1. $E(G) = \frac{1}{n(n-1)} \sum_{x \neq y \in g} \frac{1}{p(x,y)}$ demonstrates the average efficiency and $p(x,y)$ corresponds to the shortest path length between x and y. C_r and L_r relate to an identical irregular graph.

2.4. Statistical Analysis

In neuroimaging data processing, a non-parametric permutation test has been widely used and recommended. This test is based on bootstrapping, and by employing random subsets of the data, the results are validated. In this paper, the number of permutations was set to 5000, and the significance level was fixed at 5% (P-value < 0.05). It is important to note that, due to multiple comparisons and to control for Type I error, the False Discovery Rate (FDR) is applied [37]. Furthermore, there are four groups (CN, EMCI, LMCI, AD), and three different statistical tests are performed (CN vs EMCI, EMCI vs LMCI, LMCI vs AD). These comparisons follow the stages of disease progression, respectively.

3. Results

The purpose of this study is to investigate changes in brain functional graphs during the stages of AD by employing both linear and non-linear methods. Since the generating methods are different, the brain graphs vary in structure. Figure 3 depicts the brain graphs in control subjects using three different routines.

Table 1. Graph features and explanations [33-36]

Metric	Formula	Definition
Degree	-	number of edges connected to a node
Radius	$R = \min(ECC)$	-
Diameter	$D = \max(ECC)$	-
Eccentricity	$Ecc = max\{d_G(x,y)\}$	The maximal distance between a particular node and some other center point
Characteristic Path Length (CPL)	$L = \frac{\sum_{x,y \in V(G)} d_G(x,y)}{n(n-1)}$	The average distance between a node to others
Global Efficiency	$E_{glob}(G) = \frac{E(G)}{E(G^{FC})}$	Average of the inverse shortest path length
Local Efficiency	$E_{loc}(G) = \frac{1}{n} \sum_{x \in g} E(G_x)$	Global efficiency of a node. calculated on the node's neighbors
Clustering	$C = \frac{Number\ of\ closed\ triplets}{number\ of\ all\ triplets}$	A fraction of available triangles around a node
Modularity	$M = \frac{1}{l} \sum_{x,y} \left[A_{x,y} - \frac{k_x k_y}{l}\right] \delta_{x,y}$	The degree to which a graph can be partitioned into obviously isolated networks
Transitivity	$T = \frac{3 * number\ of\ triangles}{number\ of\ connected\ triples\ of\ nodes}$	The ratio of the total number of triangles to the number of triplets
Small-Worldness	$\sigma = \frac{C}{C_r} \Big/ \frac{L}{L_r}$	A small-world graph has a comparative trademark path length as an irregular graph with a similar degree conveyance yet is fundamentally more clustered

Notably, for clearer visualization, the graphs were sparsified using a 0.75 threshold

As displayed in Figure 3, each method computes and predicts functional connectivity differently. However, the variation across all methods shows more inter-modular functional connectivity in the Occipital and Frontal areas. At the same threshold, DC shows more functional connectivity compared to other methods.

In the first analysis, brain functional graphs of healthy subjects and EMCI groups are compared at different thresholds using the permutation test**.** According to the results, regardless of the selected threshold, PCC shows no significant differences. In other words, from the perspective of PCC, the modularity feature of functional brain graphs in EMCI subjects is almost the same as in healthy subjects. On the other hand, the DC method shows significant changes in the modularity feature at several thresholds. Although other thresholds show no significant difference, the P-Values are much smaller compared to PCC. The kernel-based method also shows significant changes. In comparison to DC, the kernel-based method exhibits more significant differences and has greater power to discriminate between healthy and EMCI subjects. The results are summarized in Table 2, which shows the number of significant differences for all the features in each method.

Table 2 explains that DC is more powerful than PCC and that the kernel trick is the most discriminant method overall. Regardless of the method, features such as global and local efficiencies and clustering are the most distinguishable measures, and these graph properties of the brain are the most affected characteristics when healthy subjects transition into EMCI. Sparsification is a major issue in graph analysis. The polynomial kernel highlights significant group separability due to its ability to capture non-linear dependencies in connectivity. The larger differences in clustering and modularity across groups align with biological expectations of neural disconnection in AD. Table 3 represents the effect of different thresholds. The arrays show the number of significant differences at each threshold for all the features.

As shown in Table 3, there is no exact pattern for thresholds, and the feature behaviors are non-identical. However, thresholds from 0.3 to 0.4 are the optimal values for discrimination between classes overall. It is worthwhile mentioning that the selected range for performing the investigation (0.25 to 0.75) was validated by stable graph metrics and significant separability of AD stages, ensuring biologically meaningful results. Also, the selected range aligns with the small-world network properties typical of brain connectivity. Thresholds below 0.25 often include spurious connections, while those above 0.75 may overly prune critical connections. The optimal threshold for better discrimination is approximately 0.3 to 0.4. “The threshold range of 0.3 to 0.4 was selected to balance the removal of noisy connections

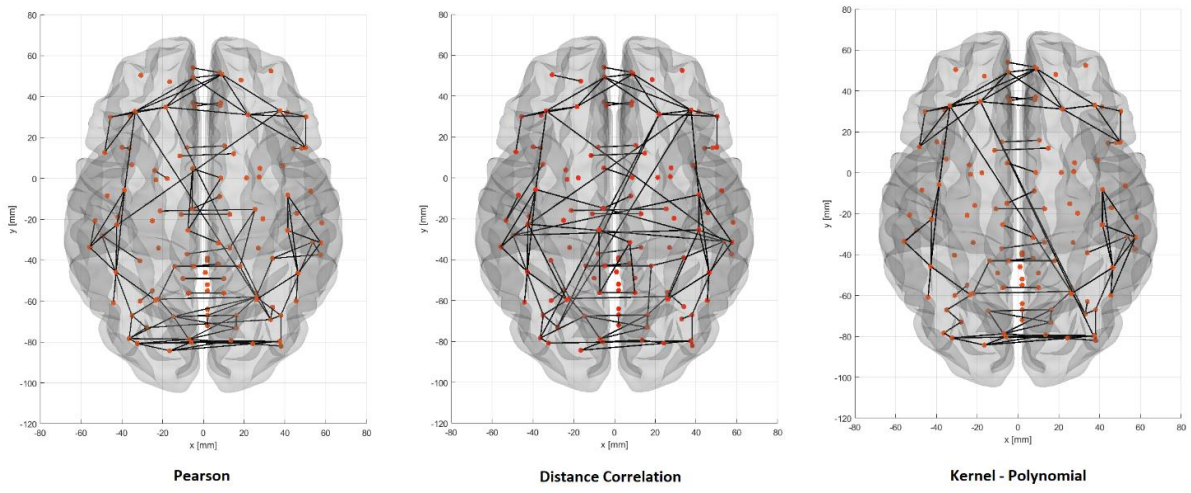

Figure 3. Demonstration of brain networks utilizing different methods in control subjects. All the graphs are sparsed with a 0.75 threshold

Table 2. Number of significant differences (P-Value < 0.05) for every feature in each method between healthy and EMCI subjects

Method Measure	Pearson Correlation (PC)	Distance Correlation (DC)	Polynomial
Degree	4	4	5
Radius	0	0	1
Diameter	1	1	2
Eccentricity	1	6	7
Characteristic Path Length (CPL)	1	4	4
Global Efficiency	6	9	8
Local Efficiency	6	6	8
Clustering	6	6	7
Transitivity	5	7	7
Modularity	0	4	8
Small-Worldness	0	7	7
Total	**30**	**54**	**64**

Table 3. Number of significant differences (P-Value < 0.05) for each feature in all the thresholds between healthy and Early Late Mild Cognitive Impairments (EMCI) subjects

Threshold Measure	0.25	0.3	0.35	0.4	0.45	0.5	0.55	0.6	0.65	0.7	0.75
Degree	0	1	1	1	1	1	1	2	2	2	1
Radius	0	0	0	0	0	1	0	0	0	0	0
Diameter	0	0	1	1	1	1	0	0	0	0	0
Eccentricity	2	2	2	2	2	2	1	0	1	0	0
Characteristic Path Length (CPL)	0	1	2	2	2	1	1	0	0	0	0
Global Efficiency	3	2	3	3	2	1	2	2	2	2	1
Local Efficiency	2	3	2	2	1	1	1	2	2	1	2
Clustering	2	2	3	2	2	2	2	1	1	1	1
Transitivity	3	3	2	2	2	3	2	1	0	0	1
Modularity	0	1	1	1	1	0	1	2	2	2	1
Small-Worldness	2	2	2	2	2	2	2	0	0	0	0
Total	**14**	**17**	**19**	**18**	**16**	**15**	**13**	**10**	**10**	**8**	**7**

while preserving biologically meaningful ones, consistent with small-world network properties observed in brain connectivity studies. This range was validated through stable graph metrics, such as clustering and efficiency, and significant group separability across AD stages. The threshold range effectively preserves meaningful connections while removing noise, as evidenced by stable graph metrics (e.g., modularity and efficiency) across all stages of AD. Results depict that the average values of modularity from PCC analysis are nearly identical in healthy (control) and EMCI subjects. Although increasing the threshold makes alterations according to the statistical test, they are not significant. As the disease progressed, EMCI subjects converted to LMCI and then AD. The approach for investigating EMCI vs. LMCI and LMCI vs. AD is the same as above. To summarize, the outputs are given in Table 4 as follows.

According to Table 4, in the EMCI vs. LMCI analysis, the non-linear methods again exhibit more power to distinguish the groups. Additionally, the kernel-based method shows better performance than the DC method. This pattern is consistent in the LMCI vs. AD examination. Between EMCI and LMCI, clustering is the most discriminative feature, followed by modularity, CPL, transitivity, and efficiencies, which illustrate significant differences. Between LMCI and AD, clustering is the most distinguishable measure, while other metrics show no significant changes. The clustering coefficient shows a

Table 4. Number of significant differences (P-Value < 0.05) for each feature in each method

Method Measure	EMCI vs. LMCI			LMCI vs. Alzheimer's Disease		
	Pearson Correlation (PC)	Distance Correlation (DC)	Polynomial	Pearson Correlation (PC)	Distance Correlation (DC)	Polynomial
Degree	0	2	4	0	1	3
Radius	1	1	1	0	0	1
Diameter	0	1	1	1	2	2
Eccentricity	0	2	2	0	0	0
Characteristic Path Length (CPL)	2	4	6	0	0	2
Global Efficiency	1	6	7	0	0	1
Local Efficiency	0	5	6	1	1	1
Clustering	5	9	11	3	4	7
Transitivity	0	6	6	0	2	6
Modularity	0	6	7	0	1	2
Small-Worldness	0	0	0	0	0	0
Total	**9**	**42**	**51**	**5**	**11**	**25**

pronounced decline from early to advanced AD stages, indicating progressive disruptions in local connectivity and functional segregation. These trends highlight the early vulnerability of specialized neural networks, such as the Default Mode Network (DMN). It is important to note that the effect of thresholding is the same as before (healthy vs. EMCI). Through a non-parametric permutation test, three different comparisons (Healthy subjects vs. EMCI, EMCI vs. LMCI, and LMCI vs. AD) are made to reveal which method can properly clarify the differences and what exactly happens to brain functional graphs as AD progresses. Table 5 summarizes the results.

Reduced values (Clustering & Modularity) indicate impaired functional segregation due to synaptic loss and neuronal death, particularly in the Default Mode Network (DMN). Modularity and clustering coefficients exhibit the most significant changes in early AD stages due to disruptions in functional brain networks caused by synaptic dysfunction and amyloid-beta accumulation. These metrics are sensitive to early connectivity changes, capturing the breakdown of network segregation and local connectivity before detectable structural damage occurs [38-40]. Declines in global efficiency show reduced long-range connectivity, while local efficiency reductions highlight disrupted short-range communication from amyloid plaques and tau pathology. These findings emphasize significant disruptions in early AD stages, underscoring the importance of early detection. The observed changes in graph metrics highlight their potential as biomarkers for early AD diagnosis, providing a non-invasive means of identifying connectivity disruptions before structural damage. Moreover, these metrics enable tracking of disease progression, offering a framework for assessing the efficacy of therapeutic interventions. The robustness of kernel-based methods supports their integration into clinical workflows, paving the way for personalized diagnostic and treatment strategies.

4. Discussion

In this study, whole-brain functional graphs were generated using PCC, the kernel trick, and DC. The graphs were sparsified with thresholds ranging from 0.25 to 0.75 (in steps of 0.05), followed by feature extraction. While PCC reveals linear dependencies, it is limited in detecting non-linear relationships. Given the brain's inherently non-linear behavior, PCC struggles to discriminate between groups based on graph features extracted from fMRI signals. Non-linear approaches, such as DC and kernel-based methods, demonstrate

Table 5. Summary of the analyses

Groups Parameter	Control vs. EMCI	EMCI vs. LMCI	LMCI vs. Alzheimer's Disease
Most discriminative features	Global and local efficiency, clustering, transitivity	Clustering	Clustering
Least discriminative features	Radius, diameter	Radius, eccentricity, diameter	Radius, eccentricity, small-worldness, Characteristic Path Length (CPL), global efficiency
Number of significant differences based on Pearson Correlation	30	9	5
Number of significant differences based on Distance Correlation	54	42	11
Number of significant differences based on Kernel	64	51	25
Optimal threshold	0.3 to 0.4	0.3 to 0.4	0.3 to 0.4

superior discriminative capability and reveal more significant connectivity changes. Among these, the kernel-based method is particularly powerful due to its ability to capture biologically meaningful, higher-order dependencies in brain connectivity. Its computational feasibility, combined with recent technological advancements, supports its potential integration into clinical workflows for early AD detection.

Although DC requires no assumptions, selecting the optimal kernel function is critical for the kernel-based method. This study utilized the polynomial kernel, as supported by prior research, due to its more effective performance in modeling complex, non-linear dependencies. The kernel method's consistent outperformance aligns with theoretical insights and empirical evidence from previous studies [7], highlighting its suitability for functional connectivity analysis, particularly in the context of neurodegenerative diseases like AD. While this study focuses on comparing well-established methods, future research will explore hybrid approaches to enhance the robustness of functional connectivity analysis.

An interesting and important result shown in Table 5 is the rate of change in the various stages of the disease. In both linear and non-linear strategies, most changes in brain functional graphs occur in the first stage of the disease. As AD progresses, the rate of variations decreases until the last stage. This pattern is consistent across all three correlation methods. Therefore, early detection of AD is crucial. The variation is completely gradual, with the minimum changes occurring as LMCI subjects convert to AD. Accordingly, in the first stage of the disease, the most discriminative features include global and local efficiency, clustering, and transitivity. These features reflect both brain functional integration and segregation. As a result, in the first stage of AD, brain functions degrade significantly. As the disease progresses and EMCI subjects transition to LMCI, the clustering metric, which represents brain functional segregation, undergoes the most significant alterations. Since features exhibiting functional integration show less modification, the overall functional decay is less evident compared to the first phase. In the transition from LMCI to AD, despite fewer alterations, clustering demonstrates the most significant changes. Hence, functional segregation continues to decline in the last stage. "The identified graph metrics provide a foundation for developing clinical decision-support tools aimed at early AD detection and monitoring. Integrating graph metrics into diagnostic workflows could offer clinicians a non-invasive, quantitative means of identifying early connectivity disruptions. These tools have the potential to complement traditional biomarkers, providing a comprehensive view of AD progression."

Clustering and Modularity reflects the breakdown of functional communities and network hubs like the DMN. Reduced global and local efficiency indicate compromised integration and local information flow,

driven by amyloid-beta and tau pathology. Metrics align with AD hallmarks such as loss of small-world properties, metabolic decline, and structural disconnections. These insights reinforce the role of graph metrics in understanding and monitoring AD progression. In summary, with the onset of Alzheimer's, the rate of variation in the brain functional graph is high, degenerating both brain functional integration and segregation. With further progression, the rate of variation declines, functional segregation is affected, and this pattern remains consistent until the last stage. On the other hand, in every stage, some features exhibit the least significant changes. Radius and diameter, which are the minimum and maximum of eccentricity, had the least discriminative potential in all stages. These metrics display the distance of a node to a specific node. Although AD degenerates the brain's functional graphs, with no significant differences, there are routes to pass between two specific nodes. In other words, nodes or ROIs are not completely and significantly isolated. This may originate from the plasticity and flexibility behaviors of the brain (human body) in confronting problems and pathological circumstances. In confirmation of previous results, as AD progresses, the number of features exhibiting no significant changes increases.

Different thresholds were evaluated to investigate the effect of thresholding in fMRI connectivity analysis. The findings demonstrate no exact patterns with threshold modifications. Nevertheless, increasing the threshold makes the graphs more sparse and lowers computational costs. As a trade-off among computational cost, meaningful characteristics, and features, and eliminating weak and spurious links, a threshold of 0.3 to 0.4 is suggested. Therefore, the best discrimination efficiency between groups in all three analyses belongs to thresholds of 0.3 to 0.4. The use of fixed sparsification thresholds has inherent limitations, including the loss of weak yet meaningful connections and sensitivity to threshold selection, as demonstrated in prior studies [41] While fixed thresholds provide computational simplicity, they may introduce bias by favoring stronger connections or affecting the stability of certain graph metrics.

5. Conclusion

Brain functional connectivity alterations in different stages of AD have been investigated via fMRI data. In comparing linear and non-linear approaches, although the non-linear ones are more complex to implement due to the brain's non-linear nature, they are recommended. While non-linear methods incur higher computational costs, their accuracy and ability to capture the brain's non-linear dynamics justify their use in AD diagnosis. Recent advancements in computational technology have made them feasible for clinical use, especially given that real-time processing is not required for AD. These methods are indispensable for detecting subtle connectivity changes, and critical for early detection and monitoring. Kernel analysis as a non-linear routine is a powerful tool wherever it can be applied, but choosing the optimal kernel function is a challenge. Although there are algorithms for determining the optimal function, trial and error remains the most prevalent method, which is one of the limitations of this research. Based on the results and the non-linear nature of the brain, investigating different non-linear methods is also recommended. Regardless of the selected analysis approaches, all of them confirmed that brain functional connectivity declines more rapidly in the early phase of AD.

Since there are no specific treatments, early detection is of great importance, and investigating the early stages of cognitive impairment and AD is recommended. As AD progresses, brain functional segregation further declines, indicating that AD adversely affects local information flow and consequently degenerates the small-world architecture of the brain. In this regard, nodal analysis of brain regions is highly recommended to reveal the most affected areas and understand how AD degenerates functional brain graphs in detail. In this study, whole-brain analysis was used, which is not comprehensive on its own; therefore, studying brain networks such as the Default Mode Network (DMN) is necessary. Another suggestion to address the limitations of this study is to investigate different statistical methods. Also, Future work will focus on hybrid methods, combining the strengths of linear and non-linear approaches to improve the precision and applicability of fMRI-based connectivity analyses. Also, Future efforts will focus on translating these findings into clinical decision-support systems, ensuring their utility in early

AD diagnosis and personalized therapeutic interventions.

References

1- Amir Abbas Tahami Monfared, Michael J Byrnes, Leigh Ann White, and Quanwu Zhang, "Alzheimer's disease: epidemiology and clinical progression." *Neurology and therapy,* Vol. 11 (No. 2), pp. 553-69, (2022).

2- M Ten Kate, F Barkhof, and Adam J Schwarz, "Consistency between Treatment Effects on Clinical and Brain Atrophy Outcomes in Alzheimer's Disease Trials." *The Journal of Prevention of Alzheimer's Disease,* Vol. 11 (No. 1), pp. 38-47, (2024).

3- Seong-Gi Kim and Peter A Bandettini, "Principles of BOLD functional MRI." in *Functional Neuroradiology: Principles and Clinical Applications*: *Springer*, (2023), pp. 461-72.

4- Mikaela Koutrouli, Evangelos Karatzas, David Paez-Espino, and Georgios A Pavlopoulos, "A guide to conquer the biological network era using graph theory." *Frontiers in bioengineering and biotechnology,* Vol. 8p. 34, (2020).

5- Jun Cao *et al.*, "Brain functional and effective connectivity based on electroencephalography recordings: A review." *Human brain mapping,* Vol. 43 (No. 2), pp. 860-79, (2022).

6- Hessam Ahmadi, Emad Fatemizadeh, and Ali Motie-Nasrabadi, "fMRI functional connectivity analysis via kernel graph in Alzheimer's disease." *Signal, Image and Video Processing,* pp. 1-9, (2020).

7- Biao Yang, Jinmeng Cao, Tiantong Zhou, Li Dong, Ling Zou, and Jianbo Xiang, "Exploration of neural activity under cognitive reappraisal using simultaneous eeg-fmri data and kernel canonical correlation analysis." *Computational and mathematical methods in medicine,* Vol. 2018(2018).

8- Gábor J Székely, Maria L Rizzo, and Nail K Bakirov, "Measuring and testing dependence by correlation of distances." *The annals of statistics,* Vol. 35 (No. 6), pp. 2769-94, (2007).

9- Hessam Ahmadi, Emad Fatemizadeh, and Ali Motie-Nasrabadi, "Deep sparse graph functional connectivity analysis in AD patients using fMRI data." *Computer Methods and Programs in Biomedicine,* Vol. 201p. 105954, (2021).

10- Hessam Ahmadi, Emad Fatemizadeh, and Ali Motie-Nasrabadi, "Multiclass classification of patients during different stages of Alzheimer's disease using fMRI time-series." *Biomedical Physics & Engineering Express,* Vol. 6 (No. 5), p. 055022, (2020).

11- Russell A Poldrack, Jeanette A Mumford, and Thomas E Nichols, Handbook of functional MRI data analysis. *Cambridge University Press*, (2024).

12- Neha Garg, Mahipal Singh Choudhry, and Rajesh M Bodade, "A review on Alzheimer's disease classification from normal controls and mild cognitive impairment using structural MR images." *Journal of neuroscience methods,* Vol. 384p. 109745, (2023).

13- Harald Hampel *et al.*, "Blood-based biomarkers for Alzheimer's disease: Current state and future use in a transformed global healthcare landscape." *Neuron,* Vol. 111 (No. 18), pp. 2781-99, (2023).

14- Shaymaa E Sorour, Amr A Abd El-Mageed, Khalied M Albarrak, Abdulrahman K Alnaim, Abeer A Wafa, and Engy El-Shafeiy, "Classification of Alzheimer's disease using MRI data based on Deep Learning Techniques." *Journal of King Saud University-Computer and Information Sciences,* Vol. 36 (No. 2), p. 101940, (2024).

15- Seyed Hani Hojjati, Ata Ebrahimzadeh, Ali Khazaee, Abbas Babajani-Feremi, and Alzheimer's Disease Neuroimaging Initiative, "Predicting conversion from MCI to AD by integrating rs-fMRI and structural MRI." *Computers in biology and medicine,* Vol. 102pp. 30-39, (2018).

16- PR Buvaneswari and R Gayathri, "Detection and Classification of Alzheimer's disease from cognitive impairment with resting-state fMRI." *Neural Computing and Applications,* Vol. 35 (No. 31), pp. 22797-812, (2023).

17- Ju-Hyeon Noh, Jun-Hyeok Kim, and Hee-Deok Yang, "Classification of alzheimer's progression using fMRI data." *Sensors,* Vol. 23 (No. 14), p. 6330, (2023).

18- Seyed Hani Hojjati, Ata Ebrahimzadeh, and Abbas Babajani-Feremi, "Identification of the early stage of Alzheimer's disease using structural MRI and resting-state fMRI." *Frontiers in neurology,* Vol. 10p. 904, (2019).

19- Emad Fatemizadeh Hessam Ahmadi, Ali Motie-Nasrabadi "A Comparative Study of Correlation Methods in Functional Connectivity Analysis using fMRI Data of Alzheimer's Patients." *Journal of Biomedical Physics and Engineering,* (2021).

20- Hessam Ahmadi, Emad Fatemizadeh, and Ali Motie-Nasrabadi, "Identifying brain functional connectivity alterations during different stages of Alzheimer's disease." *International Journal of Neuroscience,* pp. 1-13, (2020).

21- Ronald Carl Petersen *et al.*, "Alzheimer's disease neuroimaging initiative (ADNI): clinical characterization." *Neurology,* Vol. 74 (No. 3), pp. 201-09, (2010).

22- Yan Chao-Gan and Zang Yu-Feng, "DPARSF: a MATLAB toolbox for "pipeline" data analysis of resting-state fMRI." *Frontiers in systems neuroscience,* Vol. 4(2010).

23- Nathalie Tzourio-Mazoyer *et al.*, "Automated anatomical labeling of activations in SPM using a

macroscopic anatomical parcellation of the MNI MRI single-subject brain." *Neuroimage,* Vol. 15 (No. 1), pp. 273-89, (2002).

24- Jacob Benesty, Jingdong Chen, Yiteng Huang, and Israel Cohen, "Pearson correlation coefficient." in *Noise reduction in speech processing*: *Springer*, (2009), pp. 1-4.

25- Md Ashad Alam, Vince D Calhoun, and Yu-Ping Wang, "Identifying outliers using multiple kernel canonical correlation analysis with application to imaging genetics." *Computational Statistics & Data Analysis,* Vol. 125pp. 70-85, (2018).

26- Thomas Hofmann, Bernhard Schölkopf, and Alexander J Smola, "Kernel methods in machine learning." *The annals of statistics,* pp. 1171-220, (2008).

27- Martin Hofmann, "Support vector machines-kernels and the kernel trick." *Notes,* Vol. 26 (No. 3), (2006).

28- Sun Yuan Kung, Kernel methods and machine learning. *Cambridge University Press*, (2014).

29- Adam Towsley, Jonathan Pakianathan, and David H Douglass, "Correlation angles and inner products: Application to a problem from physics." *ISRN Applied Mathematics,* Vol. 2011(2011).

30- Bernhard Scholkopf and Alexander J Smola, Learning with kernels: support vector machines, regularization, optimization, and beyond. *MIT press*, (2001).

31- Olaf Sporns, "Graph theory methods: applications in brain networks." *Dialogues in clinical neuroscience,* Vol. 20 (No. 2), p. 111, (2018).

32- Brent R Logan and Daniel B Rowe, "An evaluation of thresholding techniques in fMRI analysis." *Neuroimage,* Vol. 22 (No. 1), pp. 95-108, (2004).

33- John Michael Harris, Jeffry L Hirst, and Michael J Mossinghoff, Combinatorics and graph theory. *Springer*, (2008).

34- Mikail Rubinov and Olaf Sporns, "Complex network measures of brain connectivity: uses and interpretations." *Neuroimage,* Vol. 52 (No. 3), pp. 1059-69, (2010).

35- Jeremy Kepner and John Gilbert, Graph algorithms in the language of linear algebra. *SIAM*, (2011).

36- Mark D Humphries and Kevin Gurney, "Network 'small-world-ness': a quantitative method for determining canonical network equivalence." *PloS one,* Vol. 3 (No. 4), p. e0002051, (2008).

37- Thomas E Nichols and Andrew P Holmes, "Nonparametric permutation tests for functional neuroimaging: a primer with examples." *Human brain mapping,* Vol. 15 (No. 1), pp. 1-25, (2002).

38- Mikail Rubinov and Olaf %J Neuroimage Sporns, "Complex network measures of brain connectivity: uses and interpretations." Vol. 52 (No. 3), pp. 1059-69, (2010).

39- Matthew R Brier *et al.*, "Tau and Aβ imaging, CSF measures, and cognition in Alzheimer's disease." Vol. 8 (No. 338), pp. 338ra66-38ra66, (2016).

40- Cornelis J %J Nature Reviews Neuroscience Stam, "Modern network science of neurological disorders." Vol. 15 (No. 10), pp. 683-95, (2014).

41- Hesam Ahmadi, Emad Fatemizadeh, and Ali Motie %J Frontiers in Biomedical Technologies Nasrabadi, "A comparative study of the effect of weighted or binary functional brain networks in fMRI data analysis." (2020).

.